Available online at www.sciencedirect.com
SCIENCE DIRECT
Polymer 46 (2005) 11768–11772
polymer
www.elsevier.com/locate/polymer

Nanoindentation behavior of ultrathin polymeric films

Kebin Geng [a], Fuqian Yang [a,*], Thad Druffel [b], Eric A. Grulke [a,*]

[a] Department of Chemical and Materials Engineering, University of Kentucky, Lexington, KY 40506, USA
[b] Optical Dynamics Corporation, 10100 Bluegrass Pkwy, Louisville, KY 4029p, USA

Received 27 May 2005; received in revised form 11 August 2005; accepted 31 August 2005
Available online 19 October 2005

Abstract

Measurement of the mechanical properties of nanoscale polymeric films is important for the fabrication and design of nanoscale layered materials. Nanoindentation was used to study the viscoelastic deformation of low modulus, ultrathin polymeric films with thicknesses of 47, 125 and 3000 nm on a high modulus substrate. The nominal reduced contact modulus increases with the indentation load and penetration depth due to the effect of substrate, which is quantitatively in agreement with an elastic contact model. The flow of the nanoscale films subjected to constant indentation loads is shear-thinning and can be described by a linear relation between the indentation depth and time with the stress exponent of 1/2.

Keywords: Polymeric films; Nanoindentation; Viscoelasticity

1. Introduction

Ultrathin films of polymeric materials have a number of applications, including scratch-resisting coatings, protective barriers, optical filters, and layered constructions. As examples, a scratch-resistant lens coating can improve the longevity of plastic eyeglass lenses, and multilayered nanoscale coatings with unique optical properties can be constructed to improve optical performance. In other applications, semi-permeable ultrathin layers can be used to protect surfaces from water or oxygen. In each of the applications, the physical properties of ultrathin layers, individually or in layered constructions, are difficult to determine by conventional methods such as tensile and compression tests. Similar difficulties exist in measuring the mechanical properties of quasi-one dimensional nanoscale materials such as nanotubes [1–3], nanobelts for micro-optoelectronic and biomedical applications [3–5] and nano-films [6,7]. As more applications are developed for submicron polymeric structures, there will be a greater need for direct measurements of physical properties as materials have been applied, fabricated or polymerized in place.

Studies of ultrathin polymeric films suggest that unusual properties, for example, the lower glassy–rubbery transition temperature (T_g) at near surfaces [8], are often the result of the large volume fraction of interfacial regions [9] that constitute significant portions of the material at ultrathin scales. Measurement of mechanical properties on and near polymer surfaces is likely to provide improved understanding of these unique behaviors and to improved control of the fabrication and polymerization processes of multilayer materials. In principle, there are two basic approaches for assessing viscoelastic properties of polymer surfaces; (a) contact mechanics [10,11] and (b) surface relaxation [12,13]. However, most measurements reported in literature were done on thin polymeric films with thickness more than several microns [14–16]. There are few studies of the mechanical properties of nanoscale polymeric films that include the effects of substrates, and the effects of multilayered films. In this work, we report nanoindentation studies of nanoscale polymeric films of different thicknesses (47, 125 and 3000 nm).

2. Experimental

The nanoscale polymeric films were spin-coated on silicon wafers at 1000 rpm using a spin coater (Optical Dynamic Corporation, Louisville, KY). The solution consisted of dipentaerythritol pentaacrylate from Sartomer SR399 (CAS# 60506-81-2) and 5 wt% photoinitiator 1-hydroxy-cyclohexyl-phenyl-ketone (Ciba-Geigy 184, CAS# 947-19-3), that were dissolved in equal weights of acetone and isopropanol co-solvents. The free radical reaction was initiated by dissociation of the photoinitiator molecules under UV

* Corresponding authors. Tel.: +1 859 257 8028; fax: +1 859 323 1929.
E-mail addresses: fyang0@engr.uky.edu (F. Yang), egrulke@engr.uky.edu (E.A. Grulke).

0032-3861/$ - see front matter © 2005 Elsevier Ltd. All rights reserved.
doi:10.1016/j.polymer.2005.08.096

radiation. The resulting densely cross-linked polymers exhibit good mechanical strength, thermal stability and resistance to solvent absorption, and are ideally suited as surface protective coatings and dental restorative materials [17]. SR399 is a penta-functional acrylate monomer, one of the highest functional acrylate monomers commercially available, and thus was chosen as a model monomer for this study. The thickness and surface quality of the ultrathin polymeric thin films were controlled by the solute concentration and spin speed [18,19].

All of the films were cured for 90 s in the presence of CO_2 under UV light from a germicidal lamp having an intensity of 4 mW/cm^2 at 5 cm distance. The polymerization degree or [C=C] conversion rate was monitored by Fourier transform infrared spectroscopy (FTIR) at 64 scans and resolution 4 cm^{-1} with Mattson Galaxy Series 3000 (Madison, WI). The thicknesses of the spin-coated polymer thin films were measured by a profilometer from Ambios Technology XP-1 (Santa Cruz, CA). The surface roughness of the polymeric films was determined using the tapping mode on Digital Instruments MMAFM-2 (Woodbury, NY).

The nanoindentation tests are performed in a Hysitron TriboScope (Minneapolis, MN) attached to a Quesant (Agoura Hills, CA) atomic force microscope (AFM). A diamond NorthStar cubic indenter with a nominal tip radius of 40 nm (Minneapolis, MN) is used. The penetration depth and applied load are used to compute the modulus of the films.

3. Results and discussion

The molecular structure of the SR399 monomer is shown in Fig. 1, and the FTIR spectra of the polymeric films before and after curing are depicted in Fig. 2. For comparison, the peaks at 809 cm^{-1} have been normalized in scale to the ketone peak at 1726 cm^{-1}. The extent of the reduced IR absorption of the acrylic double bond [C=C] at 809 cm^{-1} was related to the amount of polymerization [20]. The polymerization degree of this type of high functional monomer [21] was thus measured to be 76, 83 and 82% for the films of 47, 125 and 3000 nm films, respectively, which suggests that the three films were chemically similar and they were ready for mechanical comparison. The degree of polymerization is well above that needed for gelation.

The deviation of surface height from the mean plane, R_a (the arithmetic average of the absolute values), were 0.281, 0.233 and 0.250 nm for thin films of 47, 125 and 3000 nm, respectively. A typical topography of the 47 nm film is shown in Fig. 3. In general, the minimum indentation depth

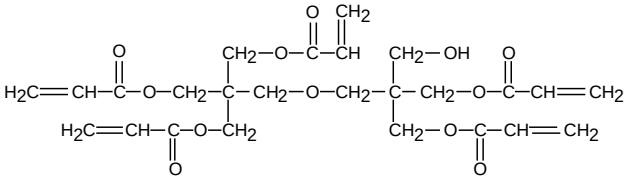

Fig. 1. Molecular structure of SR399 monomer.

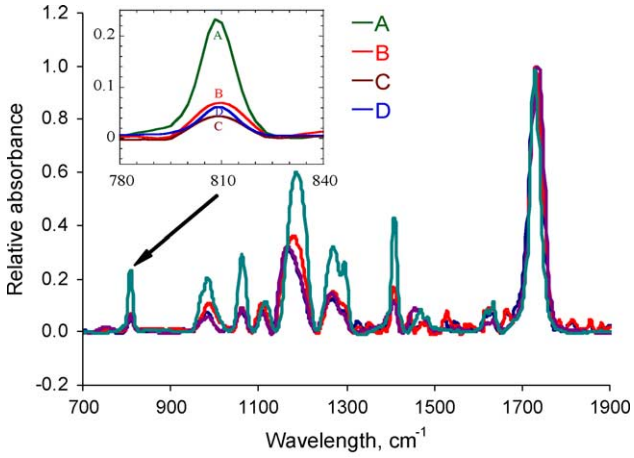

Fig. 2. The FTIR spectra of the films with different thicknesses; (a) before curing, (b) the absorbance of the 47 nm after curing, (c) the absorbance of the 125 nm after curing, and (d) the absorbance of the 3000 nm films after curing. All spectra were normalized to the peak of ketone at 1726 cm^{-1}. The absorbance of acrylic double bond at 809 cm^{-1}.

should be 20 times of R_a in order to restrict the uncertainty in contact area between the tip and the film to within 5% error [22]. Thus the minimum indentation depth required to eliminate the effect of surface roughness is about 5 nm. The smallest indentation depth in all the indentation tests was then controlled at about 5 nm.

The nanoindentation tests were carried out using the load control mode with the indentation load in the range of 0.8–100 μN. The loading rate and unloading rate were in the range of 0.16–20 μN/s. To eliminate the effect of viscoelastic deformation on the measurement of the nominal reduced contact modulus, the methodology 'held-at-peak-load' [23,24] was used. The results were averaged over more than five indentations for each testing conditions. Using the Oliver and Pharr theory [25], the reduced contact modulus, E_r, was calculated from the upper portion of the unloading curve as

$$E_r = \frac{\sqrt{\pi}}{2\sqrt{A}} \frac{dF}{d\delta} \quad (1)$$

Here, A is the contact area between the film and the indenter, F is the peak indentation load, δ is the indentation depth,

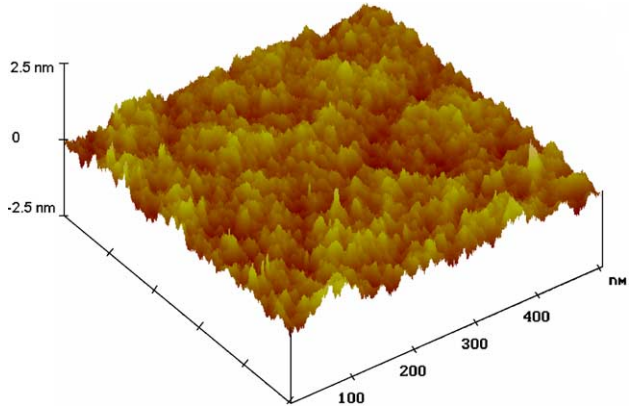

Fig. 3. AFM image of the surface of the 47 nm film.

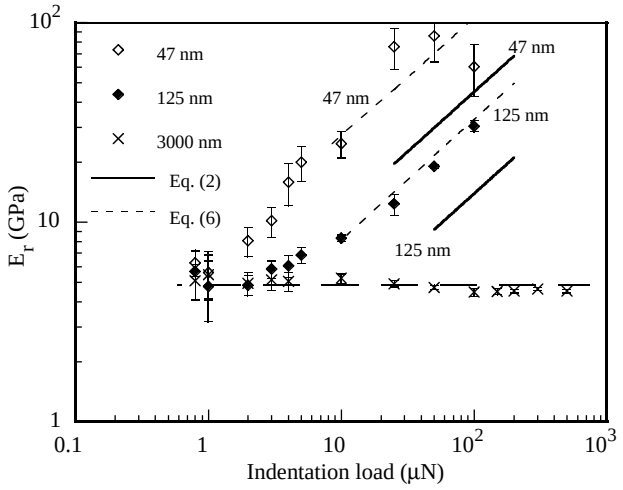

Fig. 4. Dependence of the reduced contact modulus on the indentation load.

and $dF/d\delta$ is the tangent to the upper portion of the unloading curve. No sink-in or pile-up effect was taken into account in the calculation.

Fig. 4 shows the dependence of the reduced contact modulus on the indentation load for the indentations on all three films with a holding time of 2 s. From these we see that the polymeric film of 3000 nm behaves as a bulk material relative to the films of 47 and 125 nm, and the reduced contact modulus of the 3000 nm film is 4.86 ± 0.32 GPa, independent of the indentation load. For the indentation load less than or equal to 1 μN, the reduced contact modulus are 5.62 ± 1.52 and 4.78 ± 1.60 GPa for the 47 and 125 nm films, respectively, compatible to that of the 3000 nm film. No scaling effect is observed on the behavior of surface elasticity for the nanoscale polymeric films. The measured mechanical property is consistent with the degree of polymerization monitored by the FTIR.

Fig. 5 shows the dependence of the reduced contact modulus on the indentation depth (δ) for the indentations on all three films with a holding time of 2 s, in which h is the film thickness. The reduced contact moduli for both the 47 and 125 nm films

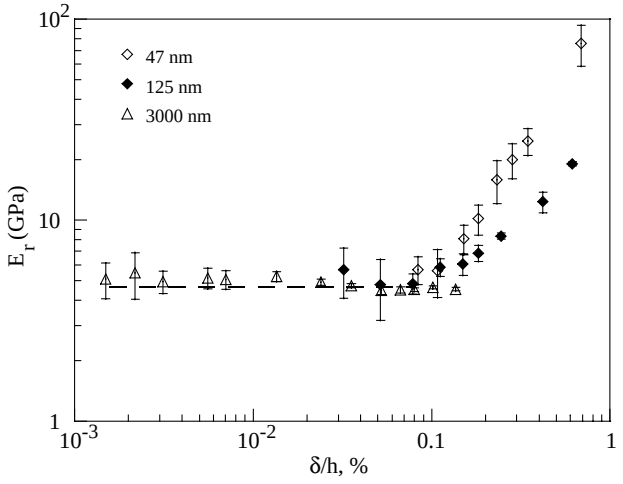

Fig. 5. Dependence of the reduced contact modulus on the indentation depth.

start to increase with the increase of the indentation depth when the indentation depth is more than 10% of the film thickness. This is due to the effect of the substrate. For the nanoscale polymeric films deposited on silicon wafers, the Young's modulus of silicon wafers is 176 GPa [26] about 37 times more than the Young's moduli of the films. Thus, the silicon substrate can be treated as a rigid substrate as compared to the polymeric films. These results support the published suggestion for indentation tests [22]—that the effect of substrate on the reduced contact modulus is negligible when the indentation depth is less than 10% of the film thickness. The reduced contact modulus is constant for an indentation depth less than 10% of the film thickness.

For the reduced contact moduli at the indentation depth over 10% of the film thickness when the substrate effect starts, we can fit the experiment data using the analytical model [27]. We approximate the cubic indenter as a conical indenter with a half included angle of 42.28° (to have the same depth to area as the cubic indenter), and assume that the polymeric films are incompressible and the contacts over the interface between the indenter and the film and that between the film and substrate are non-slip. Considering the corrected factor of 4 for non-slip contacts over both the contact interfaces for the indentation of thin films using the flat-ended indenter [28] and using the indentation load-depth relationship for the indentation of incompressible thin films with frictionless contact between the indenter and the film and the non-slip contact between the film and the substrate [27], we obtain

$$F = \frac{\pi\mu\delta^5\tan^4\theta}{5h^3}\left(\frac{3}{2}\right)^5 \tag{2}$$

Assuming that Eq. (1) can be applied to the indentation of thin films and using the relation $a = 3\delta\tan\theta/2$ for the indentation of thin films [27], one can calculate the nominal reduced contact modulus, E_r, as

$$E_r = \frac{15}{4}\frac{F^{3/5}}{\tan\theta}\left(\frac{\pi\mu\tan^4\theta}{5h^3}\right)^{2/5} \tag{3}$$

where a is the contact radius, θ the half included angle, and μ the shear modulus of the film. Assuming that the polymer is incompressible, ν_s is 0.5. For the diamond tip, E_i is 1141 GPa and ν_i is 0.07. Using the reduced contact modulus for $F \leq 1$ μN and the following equations,

$$\frac{1}{E_r} = \frac{1-\nu_s^2}{E_s} + \frac{1-\nu_i^2}{E_i} \tag{4}$$

$$\mu = \frac{E_s}{2(1+\nu_s)} \tag{5}$$

we obtain $\mu = 1.22$ GPa. Here E_s and E_i are the modulus of the film and the modulus of the tip respectively, and ν_s and ν_i are the Poisson ratios of the film and the tip respectively.

Using $\mu = 1.22$ GPa, the normal reduced contact modulus as calculated from Eq. (3) for larger indentation loads is also depicted in Fig. 4. Obviously, Eq. (3) gives the same trend as observed in the tests, although the calculated contact modulus

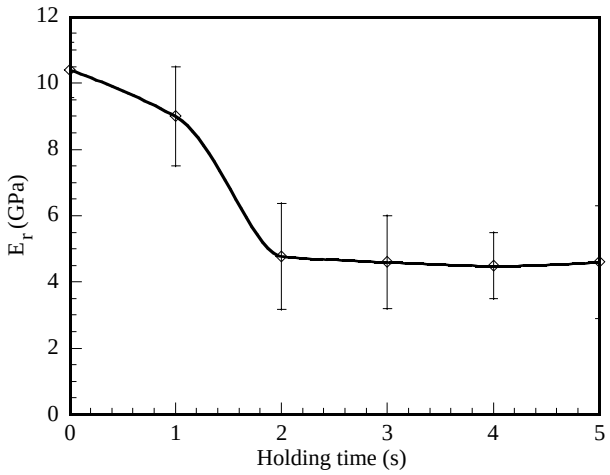

Fig. 6. Effect of the holding time on the reduced contact modulus for the indentations on the polymeric film of 125 nm with the maximum indentation load of 1 μN.

is about two times less than the experimental results. This is due to the use of the contact radius, $a = 3\delta \tan\theta/2$, in the derivation of Eq. (3). It is known that Eq. (1) is only valid for the indentation of an elastic half-space. Thus, the experimental data overestimate the nominal reduced contact modulus for the indentation of thin films at the indentation depth over 10% of the film thickness. To consider the effect of contact area on the experimental data, one needs to use the relation between the contact radius and the indentation depth, $a = 2\delta \tan\theta/\pi$, for the indentation of an elastic half-space by a conical indenter [29]. Using the same procedure in deriving Eq. (3), one obtains

$$\tilde{E}_r = \frac{3\pi}{4} E_r = \frac{45\pi}{16} \frac{F^{3/5}}{\tan\theta} \left(\frac{\pi\mu \tan^4\theta}{5h^3} \right)^{2/5} \tag{6}$$

in which $\tilde{E}_r$ is the normal reduced contact modulus using the contact area for the indentation of an elastic half-space by a conical indenter. For comparison, $\tilde{E}_r$ is also plotted in Fig. 4. Obviously, the experimental results support Eq. (6).

In general, the deformation behavior of polymers is viscoelastic. It is expected that there exists viscous flow during the indentation when subjected to a constant indentation load. To evaluate the effect of viscous flow on the unloading behavior, indentation tests were performed at a constant indentation load with different holding times between the end of the loading phase and the start of the unloading phase. Fig. 6 shows the dependence of the reduced contact modulus on the holding time for the indentations over the polymeric film of 125 nm with the maximum indentation load of 1 μN. The reduced contact modulus obtained from the unloading curves decreases with the holding time and converges to a relatively constant value of 4.78 GPa for holding times greater than 2 s. This is due to the effect of overshoot caused by the viscous flow and the inertial motion of the indenter—similar to the 'bulge' phenomenon observed in the indentation tests without holding time at smaller unloading rate [24] and verified by numerical simulation [30]. Thus, to avoid the error in the measurement of the reduced contact modulus due to the inertial force at the moment of unloading, the indenter needs to be held at the constant indentation load for a certain amount of time in order to eliminate the dynamic effect and reach the quasi-steady flow state. It should be pointed out that the holding time to reach the quasi-steady flow state is a function of the loading rate and the mechanical properties of materials. For small loading rates, the inertial force is small, and it requires less holding time for the indentation motion to attain the quasi-steady flow state. Similarly, stiffer films require less holding time.

Fig. 7 shows the time dependence of the indentation depth for the indentations on the polymeric film of 125 nm at a constant indentation load of 1 μN. The indentation depth between the end of the loading phase and the start of the unloading phase is a linear function of the holding time, which is different from the relation for Newtonian fluids [31]. The indentation velocity is independent of the indentation stress even though the indentation stress decreases with the increase of the indentation depth. It is expected that the flow behavior of the thin films is shear-thinning.

Under the quasi-steady flow state, the effect of elastic deformation on the flow behavior is negligible. The flow behavior of the polymeric films can be described as

$$\dot{\gamma} = \left(\frac{\tau}{k} \right)^n \tag{7}$$

here, $\dot{\gamma}$ is the shear rate, τ the shear stress, n the stress exponent, and k a constant (for $n = 1$, k is the viscosity). Approximating the cubic indenter as a conic indenter and using the results given by Hill [32] from the similarity analysis, one obtains

$$\int_0^t F^n \mathrm{d}t = \alpha \delta^{2n} (\cot\theta)^{2n-1} \tag{8}$$

which reduces to the result for Newtonian fluids [31]. Here α is a constant depending on k and n. Under a constant indentation load, Eq. (7) gives the time dependence of the indentation

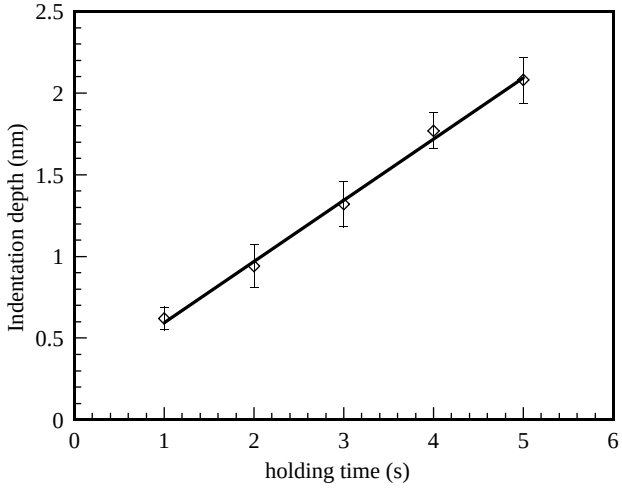

Fig. 7. Time dependence of the indentation depth for the polymeric film of 125 nm at an indentation load of 1 μN.

depth as

$$F^n \Delta t = \alpha(\cot\theta)^{2n-1}(\delta^{2n} - \delta_0^{2n}) \quad (9)$$

here δ_0 is the indentation depth before applying a constant indentation load to the indenter. When F is constant, the change in time should be directly proportional to the difference, $\delta^{2n} - \delta_0^{2n}$. Since the relation between time and indentation depth is linear as shown in Fig. 7, one obtains $n = 1/2$. Thus, the near-surface flow behavior of the nanoscale polymeric films is shear-thinning.

4. Summary

In conclusion, the deformation behavior of the SR399 nanoscale films has been evaluated using the nanoindentation technique. The reduced contact modulus increases with the indentation load due to the effect of substrate. The effect of substrate on the reduced contact modulus can be described by an elastic contact model for indentations with larger contact radius than the film thickness. Quantitative agreement between the model and the experimental results is obtained. No scaling effect was observed on the behavior of surface elasticity for the nanoscale polymeric films. The viscoelastic deformation of the films has a significant effect on the measurement of the reduced contact modulus due to the inertial motion of the indenter. It is found that there exists a critical holding time where, for times exceeding a critical holding time, the dynamic effect is negligible. The flow behavior of the SR399 nanoscale films subjected to constant indentation loading displays shear-thinning characteristics and can be described by a linear relation between the indentation depth and time with the stress exponent being 1/2.

Acknowledgements

FY is grateful for support from NSF grant DMR-0211706 and support from General Motors Corporation. KG and EG are grateful for support from Optical Dynamic Corporation.

References

[1] Pan ZW, Xie SS, Lu L, Chang BH, Sun LF, Zhou WY, et al. Appl Phys Lett 1999;74:3152.
[2] Falvo MR, Clary G, Helser A, Paulson S, Taylor RM, Chi V, et al. Microsc Microanal 1998;4:504.
[3] Wang ZL. Microsc Microanal 2004;10:158.
[4] Mao SX, Zhao MH, Wang ZL. Appl Phys Lett 2003;83:993.
[5] Yang FQ, Jiang CB, Du WW, Zhang ZQ, Li SX, Mao SX. Nanotechnology 2005;16:1073.
[6] Carneiro JO, Teixeira V, Portinha A, Dub SN, Shmegera R. Rev Adv Mater Sci 2004;7:83.
[7] Richert L, Engler AJ, Discher DE, Picart C. Biomacromolecules 2004;5:1908.
[8] Jones RAL, Richards RW. Polymers at surfaces and interfaces. Cambridge University Press: Cambridge; 1999.
[9] Teichroeb JH, Forrest JA. Phys Rev Lett 2003;91:016104.
[10] Fischer H. Macromolecules 2002;35:3592.
[11] Ge S, Pu Y, Zhang W, Rafailovich M, Sokolov J, Buenviaje C, et al. Phys Rev Lett 2000;85:2340.
[12] Hutcheson SA, McKenna GB. Phys Rev Lett 2005;94:076103.
[13] Hamdorf M, Johannsmann D. J Chem Phys 2000;112:4262.
[14] Beake BD, Leggett GJ. Polymer 2001;43:319.
[15] Li M, Palacio ML, Carter CB, Gerberich WW. Thin Solid Films 2002;416:174.
[16] Nowicki M, Richter A, Wolf B, Kaczmarek H. Polymer 2003;44:6599.
[17] Anseth KS. Polym Mater Sci Eng 1996;75:202.
[18] Meyerhofer D. J Appl Phys 1978;49:3993.
[19] Dunbar PB. J Mater Res 2001;16:145.
[20] Decker C, Jenkins AD. Macromolecules 1985;18:1241.
[21] Studer K, Decker C, Beck E, Schwalm E. Process Org Coat 2003;48:92.
[22] Fischer-Cripps AC. Nanoindentation. Berlin: Springer; 2002 p. 136.
[23] Briscoe BJ, Fiori L, Pelillo E. J Phys D: Appl Phys 1998;31:2395.
[24] Ngan AHW, Tang B. J Mater Res 2002;17:2604.
[25] Oliver WC, Pharr GM. J Mater Res 1992;7:1564.
[26] Barsoum M. Fundamentals of ceramics. New York: McGraw-Hill Comp; 1997 p. 401.
[27] Yang FQ. J Phys D: Appl Phys 2003;36:50.
[28] Yang FQ. Mech Mater 1998;30:275.
[29] Sneddon IN. Proc Cam Phil Soc 1948;44:429.
[30] Cheng YT, Cheng CM. J Mater Res 2005;20:1046.
[31] Yang FQ, Li JCM. J Non-Cryst Solids 1997;212:136.
[32] Hill R. Proc R Soc London A 1992;436:617.